ELSEVIER

Journal of Chromatography A, 772 (1997) 63–71

JOURNAL OF CHROMATOGRAPHY A

Prediction of zone patterns in capillary zone electrophoresis with conductivity detection
Concept of the zone conductivity diagram

Petr Gebauer[a,*], Jitka Caslavska[b], Wolfgang Thormann[b], Petr Boček[a]

[a]*Institute of Analytical Chemistry, Academy of Sciences of the Czech Republic, Veveří 97, CZ-611 42 Brno, Czech Republic*
[b]*Institute of Clinical Pharmacology, University of Bern, CH-3010 Bern, Switzerland*

Abstract

Conductivity detection (CD) is one of the few universal detection principles for capillary electrophoresis (important, e.g., in the detection of poorly absorbing compounds). Because of the availability of commercial instrumentation for capillary zone electrophoresis (CZE) with sensitive conductivity detection, CD in CZE became more widely used in the past few years. For the successful utilization of CD, both qualitative and quantitative aspects of the CD signal have to be recognized and understood. This requires a detailed knowledge of how the conductivity changes along an analyte zone depending on (i) the ionic mobility and dissociation constant of the analyte, (ii) the parameters of the background electrolyte used and (iii) the concentration of the analyte in its zone. This contribution is aimed at characterizing the basic properties of CD in CZE. Based on a simple theoretical treatment, the key parameters controlling the sign and magnitude of the CD signal are revealed. The concept of the limiting molar conductivity response defined as the limiting slope of the analyte zone conductivity vs. analyte concentration dependence at infinite concentration, is established. This quantity can easily be calculated for any given background electrolyte and analyte and can successfully serve for predicting the character of a CD pattern. It is shown that the sign of the limiting molar conductivity response determines the sign of the CD signal and its magnitude relates to the magnitude of the CD signal. Using a pK vs. ionic mobility coordinate system, a map of limiting molar conductivity response values can be calculated and plotted for a given CZE system. Such a diagram can be used to predict sign and magnitude of the CD response of any analyte of known ionic mobility and pK. Experimental data obtained with two commercial conductivity detectors (LKB 2127 Tachophor and AT Unicam Crystal 1000 CE) were found to agree well with theoretical predictions.

Keywords: Conductivity detection; Detection, electrophoresis; Zone patterns; Organic acids

1. Introduction

Measuring conductivity is one of the detection principles that accompanies capillary zone electrophoresis (CZE) since its establishment as a modern separation technique. Already the pioneering work of Mikkers et al. [1,2], outlining the basic principles of CZE migration and separation, was based on experiments in a PTFE capillary equipped with a conductivity detector. A boom in CZE followed the breakthrough initiated by the papers of Jorgenson and Lukacs [3–6] who operated with photometric detection. Furthermore, other very selective and/or sensitive detection techniques have become available

*Corresponding author.

PII S0021-9673(97)00103-9

recently (for a review, see, e.g., Ref. [7]). Nevertheless, conductivity detection (CD) has kept its usefulness because it represents a universal detection principle [8]. Various designs of the conductivity detector have been described [9–12] and its potential and high sensitivity have been demonstrated by practical examples [12–17]. Recently, CD has become available as part of a commercial instrument [12,13].

In a first approximation, the magnitude of the CD response can be related to the mobility difference between the analyte and the applied background electrolyte (BGE) co-ion [8]: the higher this difference is, the higher is the detection sensitivity. This holds, however, only for systems involving fully ionized monovalent ions. Moreover, the mentioned mobility difference unfortunately also controls electromigrational zone dispersion [8]. Thus, in practice, the balance between the magnitude of the detection signal and dispersion have to be optimized [12,13]. The most important factor is the proper selection of the BGE and, in particular, of its co-ion. To be successful, one should be able to predict both the level of electromigrational dispersion and the magnitude of the CD signal of the analytes of interest. Sophisticated computational procedures [18,19] can be used for this purpose, however, this use requires special training and the procedure has to be redone for each change in the sample composition. Although there is a general scheme for predicting electromigrational dispersion for both strong and weak electrolytes [20], a similar tool for predicting the magnitude of the conductivity signal is not available to date.

In this paper we present a general approach to zone conductivity in CZE. By using a simple theoretical model, we extend the concept of the molar response of a conductivity detector defined so far only for fully ionized monovalent ions [1,21] to any system comprising strong and weak electrolytes. We further introduce the concept of the zone conductivity diagram where the calculated molar responses are plotted into a pK vs. mobility coordinate system: such diagram —once made for a given BGE— allows immediate prediction of the detection response of any analyte of known ionic mobility and pK.

2. Theoretical

2.1. Strong electrolytes

Conductivity detection is based on the change in the BGE conductivity $\Delta\kappa_{BGE}$ (S m^{-1}) induced by the presence of a sample. As a measure of this change, the molar conductivity detection response b_X (S mol^{-1} m^2) was introduced for systems involving only strong monovalent ions [1,21]. It expresses the change in conductivity of the BGE induced by a change in the concentration of an analyte X ($c_{X,BGE}$) from zero to 1 M:

$$b_x = \frac{\Delta\kappa_{BGE}}{c_{X,BGE}} \tag{1}$$

In fact, b_X represents the slope of the $\Delta\kappa_{BGE}$ vs. $c_{X,BGE}$ dependence. For a simple system comprising a background electrolyte AR (consisting of a co-ion A and of a counter-ion R) and an analyte ion X (all being strong monovalent ions) only, the molar conductivity response can be expressed explicitly as [1,21]

$$b_X = F(u_X + u_R)(1 - u_A/u_X) \tag{2}$$

where u_i is the mobility of ion i and F is the Faraday constant. In this case obviously b_X is independent of concentration so that Eq. (1) can be applied using any $c_{X,BGE}$ selected. For a given BGE, the value of b_X is a function of u_X only: Fig. 1 shows a typical course of this function changing its sign at $u_X = u_A$.

When following the conductivity of an analyte zone along the separation capillary, a corresponding (spatial) peak is obtained the area of which is determined by the integral of the conductivity change along the longitudinal coordinate. For the spatial conductivity detection response of an analyte zone we thus can write

$$A_X = \int \Delta\kappa_{BGE}\, dx = n_X b_X / S \tag{3}$$

where the right-hand-side term was obtained by expressing $\Delta\kappa_{BGE}$ from Eq. (1), using $dV = S\, dx$ (V denotes volume and S the capillary cross-section which is assumed constant here) and integrating $c_{X,BGE}$ over the capillary volume by obtaining n_X as

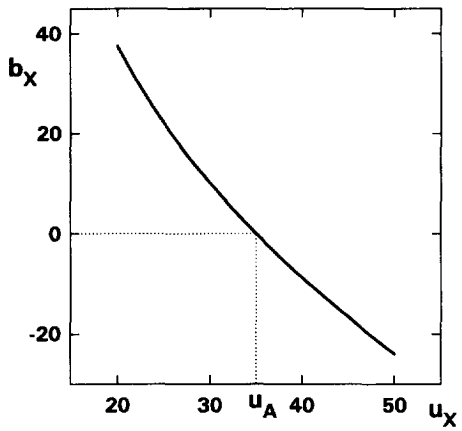

Fig. 1. Calculated dependence of the molar conductivity response, b_X (in 10^{-3} S mol^{-1} m^2), on the ionic mobility of analyte X, u_X (in 10^{-9} m^2 V^{-1} s^{-1}). The calculation according to Eq. (2) was performed using $u_A = 35 \cdot 10^{-9}$ m^2 V^{-1}s^{-1} and $u_R = 30 \cdot 10^{-9}$ m^2 V^{-1} s^{-1}.

the sampled amount of analyte X. Three conclusions follow from Eq. (3) (in agreement with [21]):

(i) A_X is directly proportional to the sampled amount n_X;

(ii) the proportionality constant differs for various analytes X only in their molar response factor b_X;

(iii) the magnitude (and sign) of b_X determines the magnitude (and sign) of A_X.

2.2. Weak electrolytes

When weak electrolytes are involved in the system and the contributions of H^+/OH^- are taken into account, the situation becomes more complex. The most important difference is that $\Delta\kappa_{BGE}$ becomes a function of the analyte concentration, $c_{X,BGE}$. Consequently, because the $\Delta\kappa_{BGE}$ vs. $c_{X,BGE}$ dependence is not a straight line here, it is no longer possible to define the molar response in the way described by Eq. (1) and to express it in the explicit way as in Eq. (2). The slope of the $\Delta\kappa_{BGE}$ vs. $c_{X,BGE}$ dependence can be generally expressed as

$$b_X = \frac{d\,\Delta\kappa_{X,BGE}}{d\,c_{X,BGE}} \quad (4)$$

We may define the limiting molar conductivity response of analyte X as

$$b_{X,0} = \left(\frac{d\,\Delta\kappa_{X,BGE}}{d\,c_{X,BGE}}\right)_{c_{X,BGE}\to 0} \quad (5)$$

i.e., as the limiting slope of the $\Delta\kappa_{BGE}$ vs. $c_{X,BGE}$ dependence for $c_{X,BGE}$ approaching zero. The quantity $b_{X,0}$ is a constant characteristic for a given analyte X and BGE; it can be simply calculated using a recently developed procedure [20] (see Section 3).

In most cases, b_x changes with the analyte concentration $c_{X,BGE}$ negligibly if restricted to dilute sample zones (which are typical in contemporary CZE practice) so that it can be approximated by $b_{X,0}$. This is demonstrated in Fig. 2 where the calculated dependence of b_X on $c_{X,BGE}$ for model analytes in the selected BGE is shown. As is seen, b_X remains almost constant up to 1 mM analyte concentrations.

When approximating the $\Delta\kappa_{BGE}$ vs. $c_{X,BGE}$ dependence to be linear for dilute sample zones, we may use $b_{X,0}$ for weak electrolytes in a similar way as b_X for strong ones and Eq. (3) can be employed for predicting the spatial peak area in the form

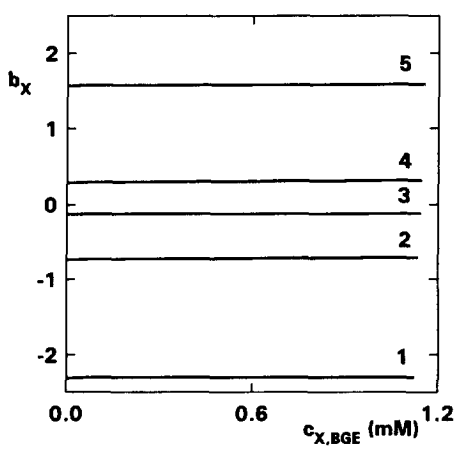

Fig. 2. Calculated dependence of the molar conductivity response (b_X, in 10^{-3} S mol^{-1} m^2) on the concentration of analyte X ($c_{X,BGE}$) in its migrating zone for model analytes of (1) $pK_{HX} = 4$, $u_X = 25 \cdot 10^{-9}$ m^2 V^{-1} s^{-1}; (2) $pK_{HX} = 3$, $u_X = 30 \cdot 10^{-9}$ m^2 V^{-1} s^{-1}; (3) $pK_{HX} = 4$, $u_X = 33 \cdot 10^{-9}$ m^2 V^{-1} s^{-1}; (4) $pK_{HX} = 0$, $u_X = 34 \cdot 10^{-9}$ m^2 V^{-1} s^{-1}; (5) $pK_{HX} = 2$, $u_X = 40 \cdot 10^{-9}$ m^2 V^{-1} s^{-1}. The BGE was 12 mM α-hydroxyisobutyric acid (HIBA) of pH 4.67.

$$A_X = n_X b_{X,0}/S \quad (6)$$

2.3. Conductivity diagram

The above presented model shows a simple way for the prediction of the CD signal. When calculating the $b_{X,0}$ values for a given BGE and for a large set of model analytes, the results can be plotted into a pK_{HX} vs. u_X coordinate system, e.g., in the form of iso-$b_{X,0}$ curves. Fig. 3 shows an example of such a plot which we call conductivity diagram (COD). The thick curve corresponds to $b_{X,0}=0$. Analytes whose $b_{X,0}$ lies on this curve do not provide a measurable conductivity response. The other curves are formed by points of analytes providing the indicated $b_{X,0}$ values. The higher the $b_{X,0}$ value, the stronger is the conductivity response of the given analyte. A positive or negative sign of $b_{X,0}$ indicates a positive or negative conductivity response, respectively. The conductivity diagram, once plotted for a given BGE, can be used for a fast and easy prediction of the conductivity response of any analyte (in this case being a strong or weak monovalent acid) of known pK_{HX} and u_X. After reading out an estimate of $b_{X,0}$, the spatial peak area can be calculated from Eq. (6).

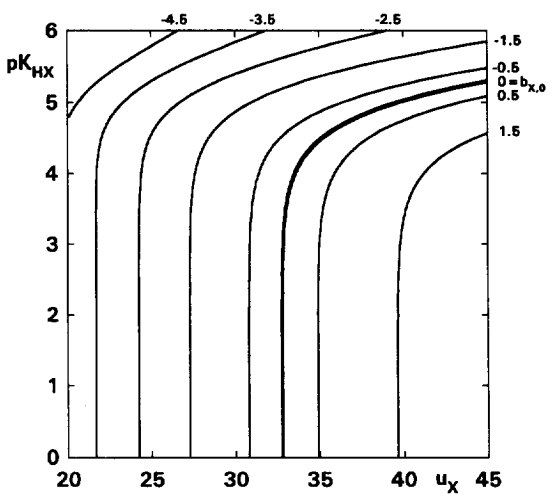

Fig. 3. Conductivity diagram for a system with 0.012 *M* HIBA + 0.01 *M* Na^+ (pH 4.67) as the BGE. The curves in the plot of pK_{HX} vs. u_X (in 10^{-9} $m^2 V^{-1} s^{-1}$) correspond to points of analytes of the indicated limiting molar conductivity response, $b_{X,0}$ (10^{-3} S mol^{-1} m^2). For further explanation, see text.

3. Experimental

For the calculation of $b_{X,0}$, a procedure was used described in detail elsewhere [20]. The model comprises a BGE composed of a weak monovalent acid HA (co-ion A^-) and a weak monovalent base B (counter-ion BH^+) with an analyte being a weak monovalent acid HX (sample anion X^-). The procedure is based on the assumption that a sample zone migrating by zone electrophoresis in a background electrolyte modifies its concentration so that all the concentrations are adjusted to keep the Kohlrausch regulating function (KRF) [18,22] constant at a given point. This means that diffusion and other dispersional effects except electromigration are neglected. Any point of a migrating sample zone is then considered to be a mixture of sample and BGE adjusted to the KRF-value of the original BGE; for a given concentration ratio of sample and BGE ions, both these concentrations can be calculated from the original BGE concentration using a set of equations expressing the regulating principle. From the concentrations, all other parameters characterizing the investigated point of the sample zone can be calculated. The calculations were made using a simple program written in QBASIC. The limiting molar conductivity response was calculated by approximating the limiting derivation described by Eq. (5) by a finite difference assuming a sample zone point with an analyte concentration as low as 60 μ*M*.

The computer simulations were performed by using a computer program based on the model of Mosher et al. [18], in its version with in situ calculation of electroosmosis [23] allowing to get both spatial and temporal zone patterns as the output. The mobilities and p*K* value used for HIBA were $33.5 \cdot 10^{-9}$ $m^2 V^{-1} s^{-1}$ and 3.97, respectively. The mobility for Na^+ was $51.9 \cdot 10^{-9}$ $m^2 V^{-1} s^{-1}$.

For the experiments, two different instruments were used. The first was a Tachophor 2127 analyzer (LKB, Bromma, Sweden) with a 28 cm×0.5 mm I.D. PTFE capillary equipped with a conductivity and absorbance detector at the column end. The measurements were performed at a constant current of 63 μA with the conductivity detector set to 10/10. The system was hydrodynamically closed so that electroosmotic flow was minimized. The data were registered with a two-channel strip chart recorder.

The second one was a Prince 300 (Lauerlabs, Emmen, Netherlands) combined with a Crystal 1000 CE conductivity detector (ATI Unicam, Boston, MA, USA). The sample was run in an untreated 50 cm × 50 μm I.D. fused-silica capillary (sample application proceeded at 20 mbar for 0.3 min) at a constant voltage of 15 kV with 50 mbar positive pressure. The polarity was set so that the migration of anions proceeded against the electroosmotic and imposed flow. For better reproducibility the capillary was rinsed between runs with 0.1 *M* NaOH, water and BGE for 5 min each.

All chemicals used were of analytical-reagent grade. Chloroacetic acid, sodium *n*-butyrate and α-hydroxyisobutyric acid (HIBA) were from Sigma (St. Louis, MO, USA). Benzoic acid, sodium salicylate, sodium glutamate and sodium hydroxide were from Merck (Darmstadt, Germany) and sodium acetate was from Fluka (Buchs, Switzerland).

A 12-m*M* solution of HIBA titrated with NaOH to a pH of 4.67 served as the BGE in all experiments. The samples were prepared by dissolving equimolar amounts of the analytes in the BGE. All solutions were prepared in deionized water. pH was measured using an Orion 720 pH meter equipped with a Ross 8103 pH electrode (both from Orion Research, Cambridge, MA, USA).

4. Results and discussion

Fig. 4 shows the conductivity diagram from Fig. 3 adapted for practical use. In addition to the parametric $b_{X,0}$ curves, there is another set of curves connecting points of analytes having the same effective mobilities ($u_{X,ef}$). The grid allows a more precise readout of the $b_{X,0}$ and $u_{X,ef}$ values from the COD. The points A to F correspond to selected model analytes referred to later on in this section. Table 1 gives their specification including their pK_{HX} and u_X values. Also shown are their calculated $b_{X,0}$ and $u_{X,ef}$ values as they correspond to Fig. 4.

From the COD, the CD characteristics of the model substances can directly be predicted. Analytes A, B, and D are expected to provide a positive detector response; analytes C, E and F should provide a negative detector response. Using the $u_{X,ef}$ network in the COD, the effective mobilities of the analytes and thus their migration (detection) order

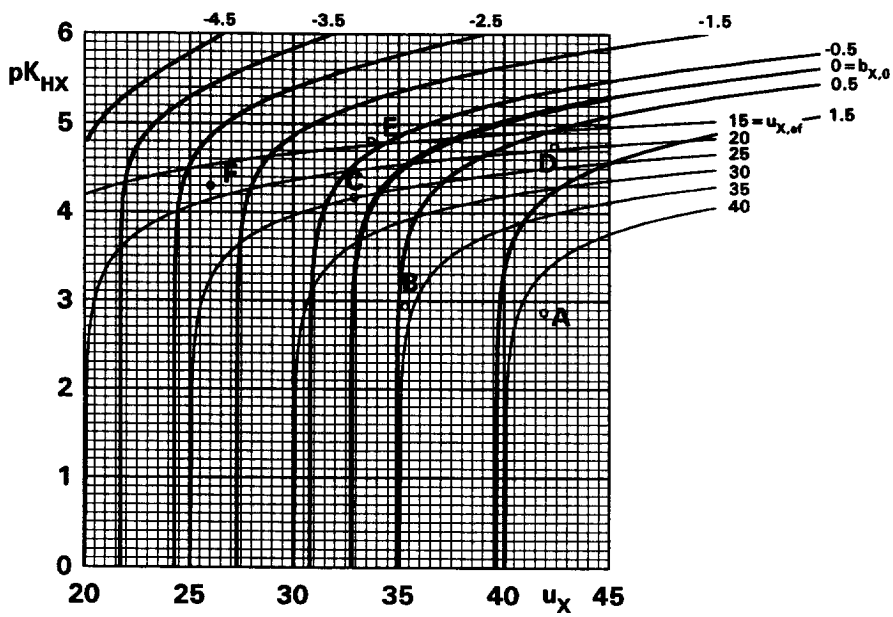

Fig. 4. The COD from Fig. 3 with the effective mobility network added. All mobility values are in 10^{-9} m^2 V^{-1} s^{-1} units. The points A to F correspond to the model analytes given in Table 1.

Table 1
Constants of the model analytes

Component X		u_X^a	pK_X	$u_{X,ef}^a$	$b_{X,0}^b$
A	Chloroacetate	41.9	2.87	41.3	1.91
B	Salicylate	35.3	2.94	34.7	0.57
C	Benzoate	32.9	4.17	25.1	−0.22
D	Acetate	42.4	4.75	19.4	0.85
E	*n*-Butyrate	33.7	4.81	14.3	−0.66
F	Glutamate	26.8	4.30	18.3	−2.07

[a] In 10^{-9} $m^2 V^{-1} s^{-1}$.
[b] In 10^{-3} $S m^2 mol^{-1}$.

can be also estimated. In the present case, this order is A (fastest), B, C, D, F, E (slowest).

Fig. 5 illustrates that the theoretical qualitative prediction is in agreement with the experiment. The sample consisted of components B, C, D and F and was run in the LKB Tachophor 2127 equipped with a conductivity detector. Despite the poor performance of this equipment including long analysis times, broad zones and considerable baseline drift, the major features of interest are clearly seen. Both the sign of the detector response and the detection order are in accordance with predictions. The experiment confirms the existence of alternating detection patterns and demonstrates that in a general case the CD signal sign and magnitude cannot be correlated with the analyte mobility or its migration order. A look at

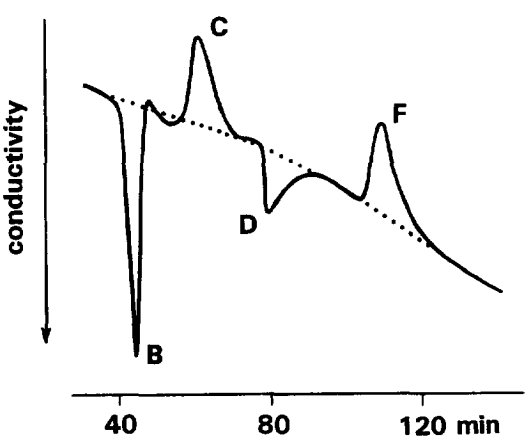

Fig. 5. Experimental conductivity record of an anionic run, showing the separation of salicylate (B), benzoate (C), acetate (D) and glutamate (F) in 0.012 *M* HIBA (pH 4.67) using the Tachophor 2127 analyzer. A 5-μl sample being 5 m*M* in B, C, D and F was introduced for the analysis. The dotted curve shows the course of the baseline.

the COD clearly shows that the existence of alternating patterns is a natural consequence of how the detection response depends on the analyte and BGE properties.

Fig. 6a shows an experiment performed in a fused-silica capillary using the Prince 300 with CD. All 6 substances of the model mixture given in Table 1 were sampled; benzoate did not provide a peak, probably due to adsorption to the capillary wall. Note that the record is of an electroosmosis driven reversed-polarity run so that the analyte of lowest effective mobility is detected first. On the record, the peak properties are well seen as far as both detection time and peak sign and magnitude are concerned: all are in good accordance with the data from the COD. Fig. 6b shows the result of a computer simulation of this system without benzoate. A good fit with the experiment is seen proving that the simulation method used provides a true picture of the real behavior of the BGE and analytes under investigation.

Computer simulation was further used to check that the calculated $b_{X,0}$ values (and/or their estimates from the COD) can also serve for predicting the conductivity signal magnitude on a quantitative level according to Eq. (6). For this, 25 min of electrophoresis of equal amounts of single substances were simulated and the spatial conductivity peak areas were plotted against the calculated $b_{X,0}$ values. Fig. 7 shows the result, demonstrating a very good linear correlation passing though the origin. Thus, although the model used for the calculation of $b_{X,0}$ involves a number of simplifications, it can serve well for the prediction of the appearance of a detection pattern even on a quantitative level.

The usual detection output consists of a signal vs. time record and for the prediction of real patterns, the spatial peak areas have to be converted into temporal ones. This can be performed simply [24] (for not too broad zones) by dividing the spatial area A_X (Eq. (6)) by the zone migration velocity $v_X = L/t_X$ (L is the effective capillary length and t_X is the detection time). The result is

$$A_{X,t} = n_X b_{X,0} t_X / V \quad (7)$$

where V is the effective capillary volume. In practice it will be sufficient to work with relative values of $A_{X,t}$ which can be calculated simply from

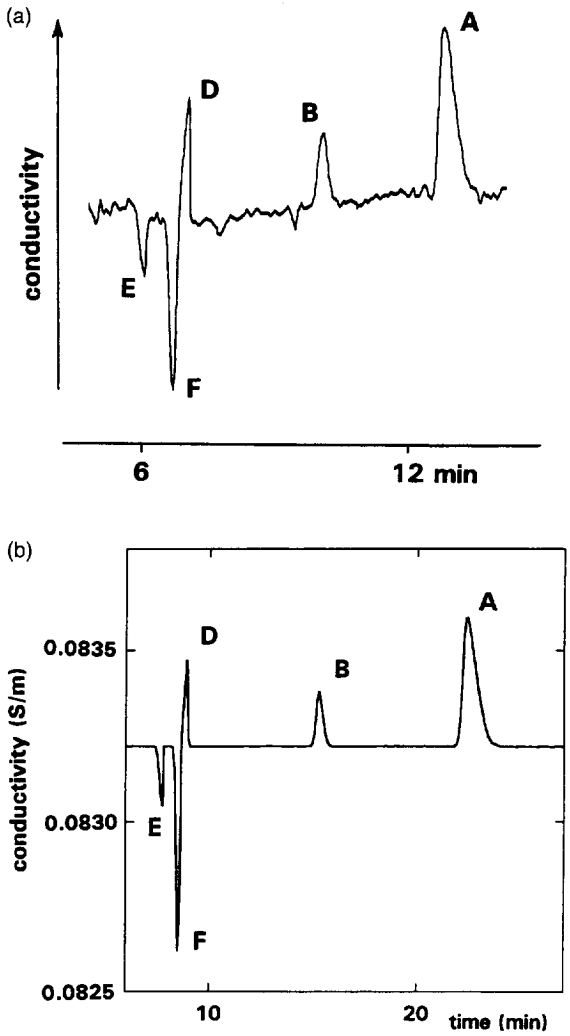

Fig. 6. (a) Experimental conductivity record of a separation of chloroacetate (A), salicylate (B), benzoate, acetate (D), glutamate (F) and *n*-butyrate (E) in 0.012 *M* HIBA (pH 4.67) using the Prince 300 apparatus. The sample was 0.5 m*M* in each of the analytes. The void peak was detected at 4.4 min of analysis time. The imposed co-flow was about 830 mm s^{-1}. (b) Computer-simulated conductivity record of a 2-mm long pulse of the same sample as (a) except benzoate. The simulation was performed for a constant voltage of 1600 V (current density changed from 666.9 A m^{-2} to 665.8 A m^{-2} over 28 min) and a 20-cm long column using 6000 segments. Electroosmotic and imposed co-flow were 137.3 and 300.0 mm s^{-1}, respectively.

$$A_{X,t,rel} = n_X b_{X,0} t_X \quad (8a)$$

or

$$A_{X,t,rel} = n_X b_{X,0} / u_{X,ef} \quad (8b)$$

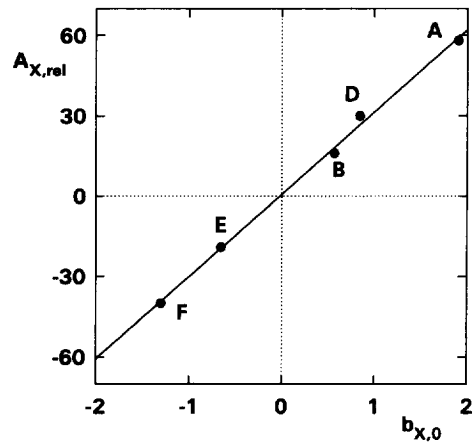

Fig. 7. Dependence of the computer-simulated spatial conductivity peak areas of the model analytes, $A_{X,rel}$ (expressed as relative values in arbitrary units) on their calculated limiting molar conductivity responses, $b_{X,0}$ (10^{-3} S mol^{-1} m^2). The simulation was performed for a constant current density of 200 A m^{-2} and a 20-cm long column using 400 segments, assuming a 4-mm long sample pulse with a concentration of 1.2 m*M*. For explanation, see text.

because t_X is inversely proportional to $u_{X,ef}$. Using Eq. (8b) the relative temporal peak areas can be calculated using only data read out from the COD (for systems with electroosmosis, the electroosmotic mobility has to be added to the read-out $u_{X,ef}$ values). For illustration, we have applied Eq. (8a) to the not overlapping experimental peaks from Fig. 6a and plotted their $A_{X,t,rel}$ against the product of calculated $b_{X,0}$ and experimental t_X (see Fig. 8). Even these few data show very good agreement with the theory: the dependence is linear and passes through the origin.

5. Conclusions

In CZE with CD, a simple prediction of the sign and magnitude of the detection signal was possible only for strong monovalent electrolytes and computer simulation was the only way to investigate more complex systems. This paper presents a simple and general way to the prediction of the CD properties of analyte zones. The concept of limiting molar conductivity response ($b_{X,0}$) is introduced as a quantity characteristic for a given analyte and BGE. It is defined (Eq. (5)) as the limiting slope of the

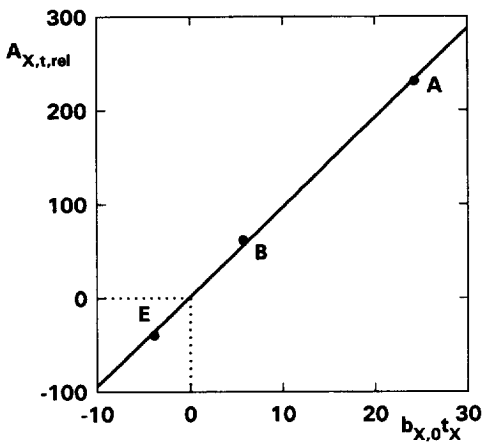

Fig. 8. Dependence of the experimental temporal conductivity peak areas of three analytes from Fig. 6a, $A_{X,t,rel}$ (expressed as relative values in arbitrary units) on the product of their calculated limiting molar conductivity response $b_{X,0}$ (10^{-3} S mol^{-1} m^2) and experimental detection time t_X (min). For explanation, see text.

dependence of BGE conductivity change on the analyte concentration for this concentration approaching zero. It is shown that for sufficiently low analyte concentrations (which is a typical case in analytical practice), the molar conductivity response is independent of the analyte zone concentration and consequently, that the conductivity peak area is directly proportional to the product of $b_{X,0}$ and the amount of sampled analyte.

The value of $b_{X,0}$ can be used to predict the sign and magnitude of an analyte peak, as well as the appearance of an entire conductivity-based detection pattern. It is useful to plot calculated $b_{X,0}$ values of analytes into a pK vs. ionic mobility coordinate system. Using a network of iso-$b_{X,0}$ curves, the sign and magnitude of the conductivity response of any analyte of known pK and mobility can be easily read out from this so-called conductivity diagram (COD). Furthermore, by inclusion of iso-effective mobility curves into the COD, the migration (detection) order of a set of analytes can be predicted, thus opening the way to the prediction of the entire detection patterns.

The described approach was verified by comparing the data with those obtained by computer simulations and experiments. Good agreement was found. The possible appearance of unusual (alternating) CD patterns predicted by the theory was demonstrated experimentally and explained as a natural consequence of the interaction between the analyte and BGE properties.

Acknowledgments

This work was supported by the Grant Agency of the Czech Republic (grants No. 203/94/0998 and 203/96/0124), the Grant Agency of the Academy of Sciences of the Czech Republic (grant No. 431404) and by the Swiss National Science Foundation.

References

[1] F.E.P. Mikkers, F.M. Everaerts, Th.P.E.M. Verheggen, J. Chromatogr. 169 (1979) 1–10.
[2] F.E.P. Mikkers, F.M. Everaerts, Th.P.E.M. Verheggen, J. Chromatogr. 169 (1979) 11–20.
[3] J.W. Jorgenson, K.D. Lukacs, Anal. Chem. 53 (1981) 1298–1302.
[4] J.W. Jorgenson, K.D. Lukacs, J. Chromatogr. 218 (1981) 209–216.
[5] J.W. Jorgenson, K.D. Lukacs, Clin. Chem. 27 (1981) 1551–1553.
[6] J.W. Jorgenson, K.D. Lukacs, J. High. Resolut. Chromatogr. Chromatogr. Commun. 4 (1981) 230–231.
[7] E.S. Yeung, Adv. Chromatogr. 35 (1995) 1–51.
[8] F. Foret, L. Křivánková and P. Boček, Capillary Zone Electrophoresis, VCH, Weinheim, 1993.
[9] F. Foret, M. Deml, V. Kahle, P. Boček, Electrophoresis 7 (1986) 430–432.
[10] X. Huang, T.K.J. Pang, M.J. Gordon, R.N. Zare, Anal. Chem. 59 (1987) 2747–2749.
[11] X.H. Huang, R.N. Zare, Anal. Chem. 63 (1991) 2193–2196.
[12] W.R. Jones, J. Soglia, M. McGlynn, C. Haber, J. Reineck, C. Krstanovic, Am. Lab. 28 (March) (1996) 25–33.
[13] C. Haber, W.R. Jones, J. Soglia, M.A. Surve, M. McGlynn, A. Caplan, J.R. Reineck, C. Krstanovic, J. Cap. Electrophoresis 3 (1996) 1–11.
[14] B. Gaš, M. Demjanenko, J. Vacík, J. Chromatogr. 192 (1980) 253–257.
[15] X. Huang, T.K.J. Pang, M.J. Gordon, R.N. Zare, Anal. Chem. 59 (1987) 2747–2749.
[16] X. Huang, J.A. Luckey, M.J. Gordon, R.N. Zare, Anal. Chem. 61 (1989) 766–770.
[17] D. Kaniansky, I. Zelenský, A. Hybenová, F.I. Onuška, Anal. Chem. 66 (1994) 4258–4264.
[18] R.A. Mosher, D.A. Saville and W. Thormann, The Dynamics of Electrophoresis. VCH, Weinheim, 1992.
[19] H. Poppe, Anal. Chem. 64 (1992) 1908–1919.

[20] P. Gebauer, P. Boček, Anal. Chem. 69 (1997) 1557–1563.
[21] M.T. Ackermans, F.M. Everaerts, J.L. Beckers, J. Chromatogr. 549 (1991) 345–355.
[22] F. Kohlrausch, Ann. Phys. Chem. 62 (1897) 209–239.
[23] R.A. Mosher, C.-X. Zhang, J. Caslavska, W. Thormann, J. Chromatogr. A 716 (1995) 17–26.
[24] S. Hjertén, K. Elenbring, F. Kilár, J.-L. Liao, A.J.C. Chress, C.J. Siebert, M.-D. Zhu, J. Chromatogr. 403 (1987) 47–61.